Probing the Interactions between cAMP and cGMP in Cyclic Nucleotide-Gated Channels Using Covalently Tethered Ligands†

Yejun He‡ and Jeffrey W. Karpen*

Department of Physiology & Biophysics, University of Colorado School of Medicine, Denver, Colorado 80262

Received August 24, 2000; Revised Manuscript Received November 1, 2000

ABSTRACT: Cyclic nucleotide-gated channels contain four ligand-binding subunits, and they are directly activated by the binding of cGMP or cAMP. Channels with different combinations of subunits are known to have different sensitivities to the two nucleotides. However, the consequences of mixed occupancy by cGMP and cAMP are not well understood, and may have important implications for understanding the functions of these channels in different cell types. We studied the activation of homomeric and heteromeric retinal rod cyclic nucleotide-gated channels with the four ligand-binding sites occupied by different combinations of cGMP (a strong agonist) and cAMP (a weak agonist). Control of occupancy was obtained by covalently tethering different numbers of cGMP moieties using the photoaffinity analogue 8-*p*-azidophenacylthio-cGMP; the remaining sites were then saturated with cAMP, or cGMP, for comparison. The fractional current activated by cAMP increased dramatically as the number of tethered cGMP moieties increased. In homomeric channels comprised of the α subunit, cAMP became an effective agonist only after three of the four sites were occupied by tethered cGMP moieties. In contrast, in heteromeric channels comprised of two α and two *β* subunits, cAMP caused significant activation after two sites were occupied by tethered cGMP moieties. In agreement with earlier work, a single residue on the *β* subunit, N1201, accounted for much of the increased efficacy of cAMP on heteromeric channels. The results are consistent with significant interactions between subunits, including the two types of subunits in heteromeric channels.

Cyclic nucleotide-gated (CNG)[1] channels play a crucial role in sensory transduction in retinal photoreceptors and olfactory receptors. In retinal rods and cones, the light-triggered hydrolysis of cGMP causes channels to close, which generates a membrane hyperpolarization (*1*−*3*). In olfactory receptor neurons, an odorant-induced rise in cAMP causes channels to open, which generates a membrane depolarization (*4, 5*). CNG channels have been detected in most other tissues, where it is likely that they cause changes in both membrane potential and Ca^{2+} entry in response to changes in cGMP and cAMP (*6*−*9*).

CNG channels contain different combinations of ligand-binding subunits that regulate their specificity and apparent affinity for cGMP and cAMP. The native rod channel is selective for cGMP (*1*); cAMP acts as a partial agonist with low apparent affinity (*10, 11*). Molecular cloning and biochemical experiments have demonstrated that the rod channel is composed of two types of subunits, α (CNCα1, CNG1) and *β* (CNC*β*1a, CNG4.1) (*12*−*20*). In heterologous expression systems, α subunits form functional homomeric channels by themselves, but several electrophysiological properties are distinct from native channels (*13*). In contrast, *β* subunits do not form functional channels when expressed on their own. However, when α and *β* subunits are coexpressed, the resulting heteromeric channels have functional properties resembling those of native channels (*17, 18*). Among these are a higher efficacy for cAMP (*21, 22*).

Several lines of evidence suggest that homomeric rod channels function as tetramers (*23*−*26*). Recent findings suggest that heteromeric channels also assemble as tetramers, with like subunits diagonally opposed in an α−*β*−α−*β* arrangement (*27*) [but see also (*21*)]. Each subunit contains a single cyclic nucleotide-binding site of about 120 amino acids near the cytoplasmic C-terminus (*13, 17, 18, 28, 29*). These sites are homologous to the corresponding regions from other known cyclic nucleotide-binding proteins, in particular the catabolite gene activator protein from *E. coli* and the regulatory subunits of cyclic nucleotide-dependent protein kinases (*30, 31*). In homomeric channels, the binding of three cGMP molecules is required for significant activation of the channel (33%), and the binding of four molecules is required for full activation (*26, 32*−*34*). Evidence also suggests that native channels require the binding of three cGMP's for significant activation (*12, 35*−*37*).

Olfactory CNG channels exhibit interesting similarities and differences. The precise subunit stoichiometry of the native channel is not known, but there is evidence for three subunit types: two that are homologous to the rod α subunit and one that is homologous to the rod *β* subunit. The subunit

† This work was supported by a grant from the National Eye Institute (EY09275 to J.W.K.).

* To whom correspondence should be addressed at the Department of Physiology & Biophysics, Campus Box C-240, University of Colorado School of Medicine, 4200 E. Ninth Ave., Denver, CO 80262. Telephone: (303) 315-8780. Fax: (303) 315-8110. E-mail: Jeffrey.Karpen@UCHSC.edu.

‡ Present address: Departments of Psychiatry and of Anatomy & Neurobiology, Washington University School of Medicine, St. Louis, MO 63110.

[1] Abbreviations: CNG, cyclic nucleotide-gated; APT-cGMP, 8-*p*-azidophenacylthio-cGMP.

10.1021/bi002014n CCC: $20.00
Published on Web 12/09/2000

most similar to the rod α subunit (CNCα3, CNG2) forms homomeric channels that are activated at much lower concentrations of cGMP than cAMP, although cAMP is a full agonist (*38*). The second α subunit (CNCα4, CNG5) (*39, 40*) and the *β* subunit (CNC*β*1b, CNG4.3) (*41, 42*), neither of which express on their own, have both been shown to increase the sensitivity of the heteromeric channel to cAMP. The coexpression of these three subunits (*41, 42*) reconstructs the behavior of the native channel, which is activated by cGMP and cAMP with similar apparent affinities (*4, 43*).

A series of studies have shown that a single residue, D604 in the rod α subunit and the corresponding residue in a number of other CNG channel subunits, plays a critical role in cyclic nucleotide specificity (*22, 44*−*47*). Changes at this position alter the ability of agonists to promote opening, with little effect on the initial binding affinity. In general, acidic residues at this position promote channel activation by cGMP, polar uncharged residues such as glutamine and asparagine decrease activation by cGMP and increase activation by cAMP, and the apolar residue methionine strongly favors activation by cAMP. The rod *β* subunit contains an asparagine at this position (N1201), while the second olfactory α subunit contains a methionine (M575). Substituting acidic residues at these positions reduces the efficacy of cAMP in heteromeric channels, particularly in the olfactory channel (*22, 47*). It is clear, however, that other parts of CNG channel subunits can also make an important contribution to the overall efficacies of cGMP and cAMP (*22, 48*).

There is reason to believe that cGMP and cAMP simultaneously regulate the opening of CNG channels in a number of cell types. In this vein, we were intrigued by earlier studies showing that low concentrations of cAMP, which caused little or no activation of native retinal rod channels, potentiated cGMP-induced currents (*49, 50*). This effect has recently been reproduced in expressed heteromeric channels, and shown to be influenced strongly by *β*-N1201 (*22*). In this study, we have examined the interactions between cGMP and cAMP in more detail in homomeric and heteromeric rod CNG channels, employing a technique for covalently tethering cGMP moieties to the binding sites of the channel using the photoaffinity analogue 8-*p*-azidophenacylthio-cGMP (APT-cGMP) (*28, 51*). This approach was used successfully in the past to lock channels in partially liganded states and assess their behavior, without the ambiguities that arise from continuous binding and unbinding of ligands to channel subunits (*26, 33, 52*). Here the method was used to study channel activation with the four binding sites occupied by defined combinations of cGMP and cAMP. The results show that cAMP becomes an effective agonist when channels are primed by the binding of cGMP. Furthermore, homomultimers and heteromultimers require different numbers of bound cGMP's to cause a substantial increase in cAMP efficacy.

MATERIALS AND METHODS

Molecular Biology. Full-length cDNA clones of the α (*13*) and *β* (*18*) subunits of the bovine retinal rod CNG channel were subcloned into the pGEM-HE vector, a high-expression vector in *Xenopus laevis* oocytes (*53*). The point mutation, *β*-N1201D, was generated with the QuikChange Site-Directed Mutagenesis Kit (Stratagene, La Jolla, CA). Messenger RNAs were transcribed in vitro with the mMESSAGE mMACHINE T7 Kit (Ambion, Austin, TX) and microinjected in *Xenopus* oocytes. Typically, each oocyte was injected with 50 nL of total mRNA at a concentration of 0.5−10 ng/nL. For heteromeric channel expression, we normally used a 1:2.5 molar ratio of α to *β* subunit mRNA. It has been shown previously that this ratio strongly favors the formation of heteromeric channels (*21, 27*). After injection, the oocytes were incubated at room temperature (21−23 °C) overnight, and subsequently at 18 °C. Electrophysiological recordings were carried out from 2 to 14 days after injection.

Electrophysiology. Patch clamp recordings of channel activity were performed on excised inside-out membrane macropatches, using an Axopatch 1D amplifier (Axon Instruments, Foster City, CA). Recordings were at room temperature. Electrodes had resistances of 0.7−1.5 MΩ. Currents were usually evoked by 200-ms pulses to +50 mV from a holding potential of 0 mV. Some experiments were done at −50 mV for comparison, and this did not alter any of the conclusions. The currents were low-pass filtered at 1 kHz with an eight-pole Bessel filter (Frequency Devices, Haverhill, MA), and sampled at 5 kHz. Currents at low cyclic nucleotide concentrations were measured at steady state, whereas currents at high cyclic nucleotide concentrations were measured 2 ms after switching the voltage to minimize ion accumulation and depletion effects (*54*). Currents larger than 5 nA were corrected for the voltage drop across the pipet series resistance. Data were acquired and analyzed with pCLAMP 6 software (Axon Instruments). In some experiments, solutions were applied to the macropatches using an RSC-100 rapid solution changer (Molecular Kinetics, Pullman, WA). The solution in the patch pipet and experimental chamber contained (in mM): 130 NaCl, 2 Hepes (pH 7.6), 0.02 EDTA, and 1 EGTA. Different concentrations of cyclic nucleotides, including cGMP, cAMP, and cIMP (Sigma, St. Louis, MO), were added to the cytoplasmic side of the membrane patch. The channel blocker L-*cis*-diltiazem, which selectively blocks heteromeric channels at 10 *μ*M (*17, 18, 55, 56*), was used to confirm heteromeric channel formation. To determine dose−response relations before covalent activation, leak currents in the absence of cyclic nucleotide were subtracted. The relations were measured at least 10 min after patch excision, to avoid the spontaneous changes in cyclic nucleotide sensitivity that can occur early in a patch (*57*). The fraction of maximal current, I/I_{max}, is the ratio between the current at a given concentration of cyclic nucleotide and the maximal current induced by a saturating concentration. All dose−response relations were fit with the Hill equation: $I/I_{max} = [\text{cyclic nucleotide}]^n/([\text{cyclic nucleotide}]^n + K_{1/2}{}^n)$, where n is the Hill coefficient and $K_{1/2}$ is the concentration of cyclic nucleotide that gives a half-maximal current. Curve fitting and plotting were done using Sigma Plot software (Jandel Corp., San Rafael, CA).

The synthesis of APT-cGMP and the method of covalent activation of CNG channels have been described in detail (*51*). In brief, patches exposed to 20 *μ*M APT-cGMP (a nearly saturating concentration) were illuminated with long-wavelength UV light (centered at 360 nm) from a 200-W mercury lamp for different amounts of time. After exposure, patches were washed extensively with cyclic nucleotide-free control solution for at least 15 min to remove all untethered

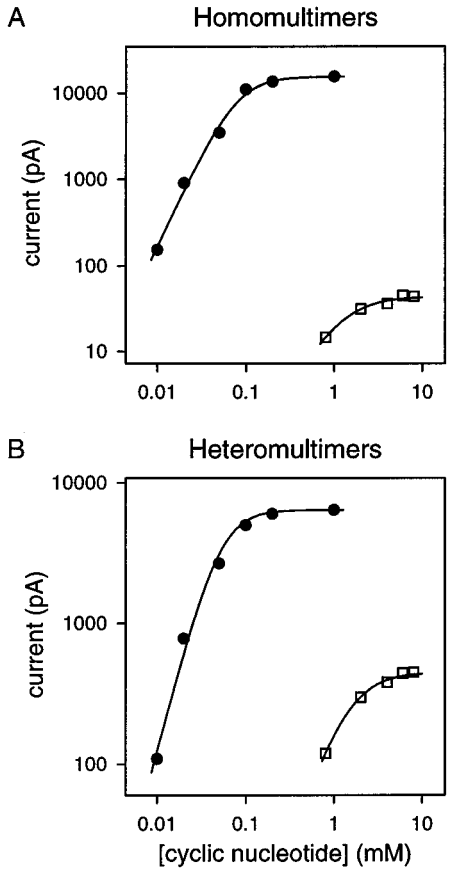

FIGURE 1: cAMP is a partial agonist for rod CNG channels. Double logarithmic plots of cGMP (circles) and cAMP (squares) dose−response relations obtained from the same macropatch expressing either homomeric (A) or heteromeric (B) channels. Smooth curves are fits to the Hill equation (see Materials and Methods). (A) cGMP, $n = 2.2$, $K_{1/2} = 79$ μM, $I_{sat.\ cG} = 15\,644$ pA; cAMP, $n = 1.7$, $K_{1/2} = 1.2$ mM, $I_{sat.\ cA} = 44$ pA. (B) cGMP, $n = 2.4$, $K_{1/2} = 52$ μM, $I_{sat.\ cG} = 6421$ pA; cAMP, $n = 1.9$, $K_{1/2} = 1.4$ mM, $I_{sat.\ cA} = 447$ pA.

nucleotide. To determine the persistent current through the CNG channels, the leak current was measured by perfusing the patch with 5 mM $MgCl_2$, which blocks 96−98% of the Na^+ current through the channels (*26*, *28*). The level of covalent activation was expressed as I_p/I_{max}, the persistent current divided by the maximal patch current. To obtain a dose−response relation for free cyclic nucleotide atop a level of covalent activation, the persistent current was subtracted from the total currents in the presence of different concentrations of cyclic nucleotide.

Reduced Chi-Square Test. The reduced chi-square test (*58*) was used to evaluate the goodness of fits. Reduced chi-square, χ_v^2, is the ratio of the estimated variance (variance of the fit) to the parent variance (variance of the data). We used a five-point sliding window to estimate the variance of the center datum. This was done with MATLAB software (The Math Works, Inc., Natick, MA). The variances of the first two and last two data were assigned the same value as that of the third and third to last data, respectively. A χ_v^2 value near unity was interpreted as a good fit.

RESULTS

Partial Agonists Become Much More Potent in Activating Rod CNG Channels with One or More cGMP's Tethered. Figure 1 shows cGMP and cAMP dose−response relations for homomeric and heteromeric rod channels expressed in *Xenopus* oocytes. In agreement with earlier studies (*10*, *11*, *21*, *22*, *44*), cAMP was a partial agonist that activated only a small percentage of the current activated by cGMP. In addition, the cAMP concentration that elicited a half-maximal current was also much higher. The cAMP-induced currents through both homomeric and heteromeric channels reached a maximum at 8 mM, which was used in later experiments as the saturating cAMP concentration. On average, saturating cAMP elicited about 0.7% of the maximal cGMP-induced current (i.e., $I_{sat.\ cA}/I_{sat.\ cG} = 0.7\%$) from homomeric channels and about 6% from heteromeric channels (Table 1). Thus, cAMP is a more effective agonist of heteromeric channels, apparently due to a more favorable interaction with β subunits (*11*, *21*, *22*).

Table 1: cGMP and cAMP Activation Parameters for Different CNG Channel Constructs[a]

	cGMP		cAMP		
	n	$K_{1/2}$ (μM)	n	$K_{1/2}$ (mM)	$I_{sat.\ cA}/I_{sat.\ cG} \times 100$
α	2.0 ± 0.4 (19)	72 ± 25 (19)	2.0 ± 0.9 (17)	1.2 ± 0.5 (17)	0.7 ± 0.5 (70)
α + β	2.2 ± 0.4 (36)	74 ± 18 (36)	1.9 ± 0.7 (41)	1.2 ± 0.5 (41)	6.0 ± 4.6 (83)
α + βN1201D	2.4 ± 0.5 (17)	81 ± 25 (17)	1.9 ± 0.8 (11)	1.2 ± 0.6 (11)	1.4 ± 1.0 (17)

[a] n and $K_{1/2}$ (Hill equation parameters) are defined under Materials and Methods; $I_{sat.\ cA}/I_{sat.\ cG}$ is the ratio between the current induced by saturating cAMP and the current induced by saturating cGMP. Values are expressed as mean ± SD. Number of experiments is indicated in parentheses.

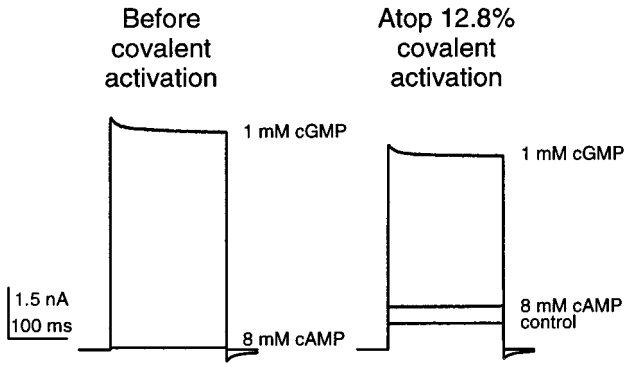

FIGURE 2: cAMP becomes a much more effective agonist for rod CNG channels atop covalent activation (achieved by photolysis of APT-cGMP). Leak-subtracted currents elicited by saturating cGMP (1 mM) and saturating cAMP (8 mM) through homomeric channels are shown before covalent activation (left) and atop 12.8% covalent activation [a persistent current in cyclic nucleotide-free control solution that was 12.8% of the maximal patch current (right)]. Currents were evoked by +50-mV pulses from a holding potential of 0 mV. Before covalent activation, the ratio between the current induced by saturating cAMP and the current induced by saturating cGMP, $I_{sat.\ cA}/I_{sat.\ cG}$, was 0.84%; atop 12.8% covalent activation, $I_{sat.\ cA}/I_{sat.\ cG}$ increased to 8.4%.

Cyclic AMP became a much more effective agonist of rod CNG channels after one or more cGMP moieties were covalently tethered. Exposure of patches to APT-cGMP and UV light for increasing amounts of time causes progressive covalent activation of rod CNG channels (*28*, *51*, *52*). For the homomultimers shown in Figure 2, atop 12.8% covalent activation (a persistent current in cyclic nucleotide-free control solution that was 12.8% of the maximal patch current

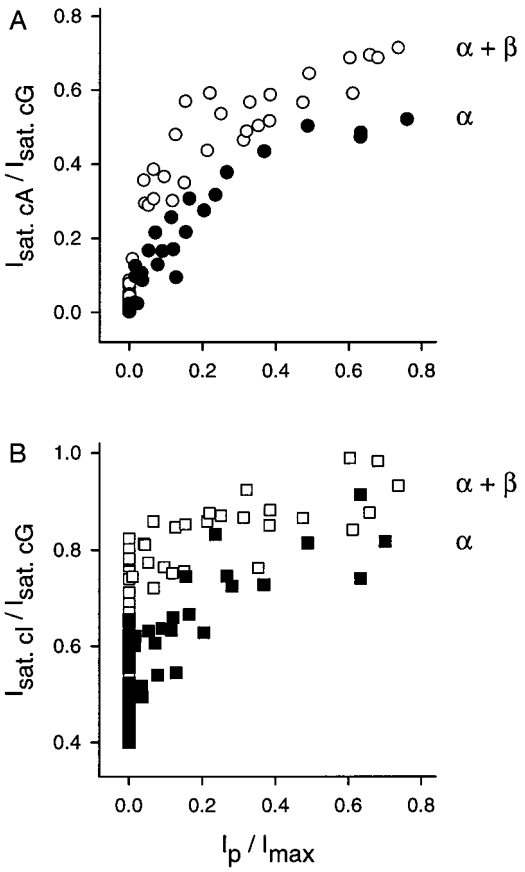

FIGURE 3: Efficacy of partial agonists depends on the level of covalent activation. (A) The ratios between the current induced by saturating cAMP and the current induced by saturating cGMP ($I_{sat.\ cA}/I_{sat.\ cG}$) through homomeric (filled circles) and heteromeric (open circles) rod CNG channels are plotted against the level of covalent activation (I_p/I_{max}: the persistent current divided by the maximal patch current). Although there was some data scatter before covalent activation, the maximal cAMP response increased with increasing levels of covalent activation in every patch (as shown in the examples in Figure 4). (B) The ratios between the current induced by saturating cIMP and the current induced by saturating cGMP ($I_{sat.\ cI}/I_{sat.\ cG}$) through homomeric (filled squares) and heteromeric (open squares) channels are plotted against the level of covalent activation. Similarly, although there was some data scatter, the maximal cIMP response increased with increasing levels of covalent activation in every patch. Note, the different ordinate scales in (A) and (B).

in saturating cGMP, i.e., $I_p/I_{max} = 12.8\%$), saturating cAMP evoked about 8.4% of the remaining activatable current ($I_{sat.\ cA}/I_{sat.\ cG} = 8.4\%$), compared to 0.84% before permanent activation. There was a small change in the maximal patch current, but this was not a consistent phenomenon, and did not affect the observation of "priming" by covalently tethered cGMP. The maximal cAMP responses of both homomeric and heteromeric channels increased dramatically with increasing levels of covalent activation (Figure 3A, where $I_p/I_{max} > 0$). As was true in the absence of bound cGMP, cAMP was a more effective partial agonist for heteromultimers than for homomultimers at all levels of covalent activation. Atop 75% covalent activation, saturating cAMP evoked about 50% of the maximal cGMP-induced current through the remaining channels in homomultimers and about 70% in heteromultimers. Thus, cAMP can become an effective agonist when channels are first primed (partially liganded) by cGMP. Because we applied a saturating concentration of cAMP, the increase in activation efficacy is not due to an increase in ligand-binding affinity. It is also unlikely to result from a change in channel conductance, based on a previous study which showed that the single-channel conductance of the native bovine channel is similar in cGMP and cAMP (*50*). Rather, the increased cAMP efficacy is likely due to an increase in the probability of opening.

We next tested the efficacy of cIMP, whose structure is intermediate between cGMP and cAMP, atop different levels of covalent activation. Cyclic IMP is also a partial agonist of the rod CNG channel, but more effective than cAMP (*10*, *44*). Saturating cIMP (8 mM) elicited about 50% of the maximal cGMP-induced current from homomultimers and about 65% from heteromultimers (Figure 3B, where $I_p/I_{max} = 0$). Similar to cAMP, the cIMP efficacy improved atop covalent activation (Figure 3B, where $I_p/I_{max} > 0$). Thus, the efficacy of both partial agonists depends on the number of covalently tethered cGMP molecules.

We also verified that shifts in the dose−response relations for free cyclic nucleotide were occurring after covalent activation (Figure 4). In this case, $I/I_{sat.\ cG}$ represents the increase in current caused by free cyclic nucleotide nomalized by the maximal increase caused by saturating cGMP (atop the level of persistent current). The cGMP dose−response relations changed in two respects atop covalent activation, as previously reported (*52*). First, $K_{1/2}$ (the concentration that caused a half-maximal increase in current) was lower because the probability that the channels would be fully liganded at any given cGMP concentration was higher. Second, n was lower because fewer free ligands were required to activate the channels. The cAMP dose−response relations atop covalent activation were less complete, but it is clear that in addition to the large increase in efficacy at saturating concentrations, $K_{1/2}$ was also shifted to lower concentrations as expected (Figure 4). Similar changes were observed in cIMP dose−response relations (data not shown).

Dissecting the Number of Tethered cGMP Molecules Required to Substantially Increase the Efficacy of cAMP in Homomeric and Heteromeric Channels. An advantage of covalently tethering cGMP moieties is that the effects of defined combinations of bound cGMP and cAMP can be assessed. We can estimate with some accuracy in macropatches the distribution of liganded states at a particular level of covalent activation. This analysis, given below, is based on previous studies at the single-channel level in which channels were locked in each possible liganded state and the degree of opening was measured (*26*, *33*). Furthermore, cAMP can be added at saturating concentrations to occupy the remaining binding sites, without the complication of the two ligands competing. Both theoretical and experimental arguments support this. First, the extended (maximal) length of the linker chain in APT-cGMP is <10 Å so that the effective concentration of an unbound, but tethered, cGMP moiety is expected to be on the order of hundreds of millimolar. Second, the addition of saturating concentrations of cGMP (*26*) or cAMP did not increase or decrease the current through fully tethered channels.

To quantify the effects of tethering one to three cGMP moieties on cAMP efficacy, the cAMP data for homomultimers and heteromultimers in Figure 3A are replotted separately in Figure 5. Each level of persistent current on the abscissa (I_p/I_{max}) defines a distribution of liganded states

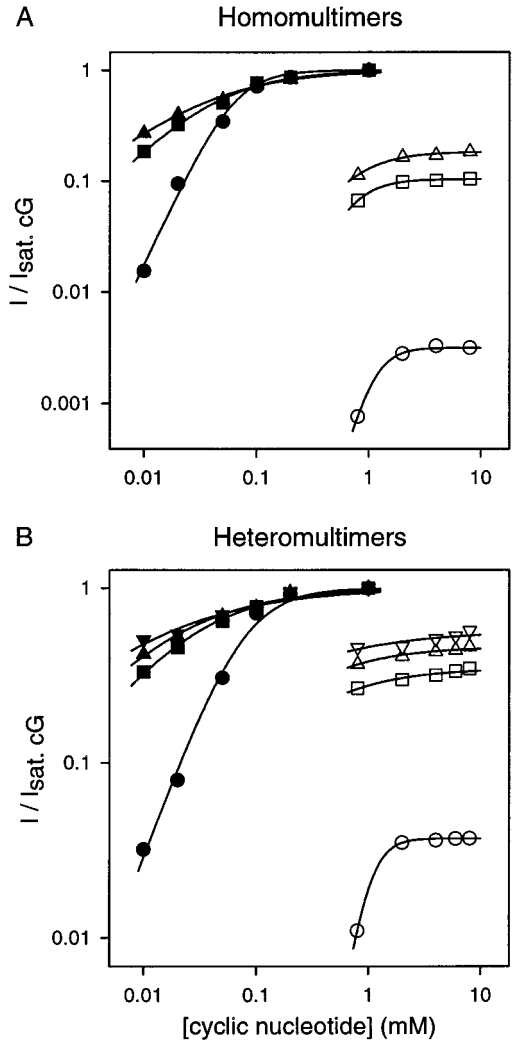

FIGURE 4: Double logarithmic plots of cGMP (filled symbols) and cAMP (open symbols) dose−response relations for homomeric (A) and heteromeric (B) rod CNG channels atop different levels of covalent activation. At each level of covalent activation, the currents induced by free cyclic nucleotide were normalized by the maximal current induced by saturating cGMP ($I/I_{sat.\ cG}$). Smooth curves are fits to the Hill equation as in Figure 1. (A) Circles, data before covalent activation; squares, data atop 1.7% covalent activation; upward triangles, data atop 5.3% covalent activation. Before covalent activation: cGMP, $n = 2.2$, $K_{1/2} = 62\ \mu$M; $I_{sat.\ cA}/I_{sat.\ cG} = 0.33\%$. 1.7% covalent activation: cGMP, $n = 1.1$, $K_{1/2} = 41\ \mu$M; $I_{sat.\ cA}/I_{sat.\ cG} = 10.5\%$. 5.3% covalent activation: cGMP, $n = 0.8$, $K_{1/2} = 33\ \mu$M; $I_{sat.\ cA}/I_{sat.\ cG} = 18.4\%$. (B) Circles, data before covalent activation; squares, data atop 4.0% covalent activation; upward triangles, data atop 12.6% covalent activation; downward triangles, data atop 21.9% covalent activation. Before covalent activation: cGMP, $n = 1.8$, $K_{1/2} = 75\ \mu$M; $I_{sat.\ cA}/I_{sat.\ cG} = 3.70\%$. 4.0% covalent activation: cGMP, $n = 0.9$, $K_{1/2} = 23\ \mu$M; $I_{sat.\ cA}/I_{sat.\ cG} = 34.8\%$. 12.6% covalent activation: cGMP, $n = 0.8$, $K_{1/2} = 16\ \mu$M; $I_{sat.\ cA}/I_{sat.\ cG} = 46.3\%$. 21.9% covalent activation: cGMP, $n = 0.6$, $K_{1/2} = 11\ \mu$M; $I_{sat.\ cA}/I_{sat.\ cG} = 57.1\%$.

(zero to four tethered cGMP's). To calculate this distribution, we assumed that covalent attachment of ligands to the channel's binding sites in both homomultimers and heteromultimers was a random process, for the following three reasons. First, a nearly saturating concentration of APT-cGMP (20 μM) was used, so that almost all of the binding sites were occupied. This helped to ensure that covalent attachment of ligands was not influenced by binding-site affinities. Second, it was shown previously that the time-courses for covalent activation of native channels and expressed homomeric channels were very similar, which argues that the two subunits of the native channel label with similar efficiency (*52*). Third, covalent attachment of ligands at all but one site of native rod channels (*52*) and expressed heteromeric channels (unpublished data) revealed a functional heterogeneity in the ligand-binding sites (two populations in roughly equal proportion, that bound cGMP with apparent affinities that differed by a factor of ~25). This finding makes it likely that covalent attachment at the two different types of sites occurred with similar efficiencies. Otherwise, a high proportion of channels would have been missing ligands at the class of site in which covalent attachment was more difficult, resulting in a nearly homogeneous population of unoccupied sites. If covalent attachment is a random process, the probability that a channel will contain a certain number of covalently tethered ligands (x) is given by the binomial distribution:

$$f(x) = n!/[(n - x)!x!]p^x q^{n-x} \quad (1)$$

where n is the total number of ligand-binding sites, p is the probability that a particular site is labeled, and q is the probability that a particular site is not labeled ($1 - p$). As described earlier, there is evidence that rod CNG channels are tetramers; thus, we assumed $n = 4$. In an earlier study of single homomeric channels locked in different ligand-bound states using APT-cGMP (*26*), triply liganded channels produced 33% as much current as fully liganded channels and doubly liganded channels produced 1%, while singly liganded and unliganded channels produced about 0.001%. To calculate p, we assumed that channels with less than three ligands attached made a negligible contribution to the persistent current. Under those conditions

$$I_p/I_{max} = f(4) + 0.33\, f(3) \quad (2)$$

Substituting $f(4) = p^4$, and $f(3) = 4p^3(1 - p)$ from eq 1 yields

$$I_p/I_{max} = 1.3p^3 - 0.3p^4 \quad (3)$$

At each value of I_p/I_{max} in Figure 5, p was calculated from eq 3, and the fraction of channels with zero to three cGMP's tethered, $f(x)$, was then calculated from eq 1. The amount of current through each liganded state of the channel has not been determined in heteromeric channels, but the distribution of liganded states is not likely to deviate significantly from that calculated using eqs 1−3 for three reasons. First, the mean Hill coefficients for activation of single channels are not measurably different between homomeric and heteromeric channels (*34*). Second, like homomeric channels, heteromeric channels have at least one subconductance state that is prominent in partially liganded channels (*59*). Third, the biggest uncertainty in heteromeric channels is the precise contribution of partially liganded channels to the current, but the calculation above is dominated by the contribution of fully liganded channels.

With $f(0)$, $f(1)$, $f(2)$, and $f(3)$ defined at each value of I_p/I_{max}, the data in Figure 5 were fit with the following equation:

$$I_{sat.\ cA}/I_{sat.\ cG} = a\, f(0) + X\, f(1) + Y\, f(2) + Z\, f(3) \quad (4)$$

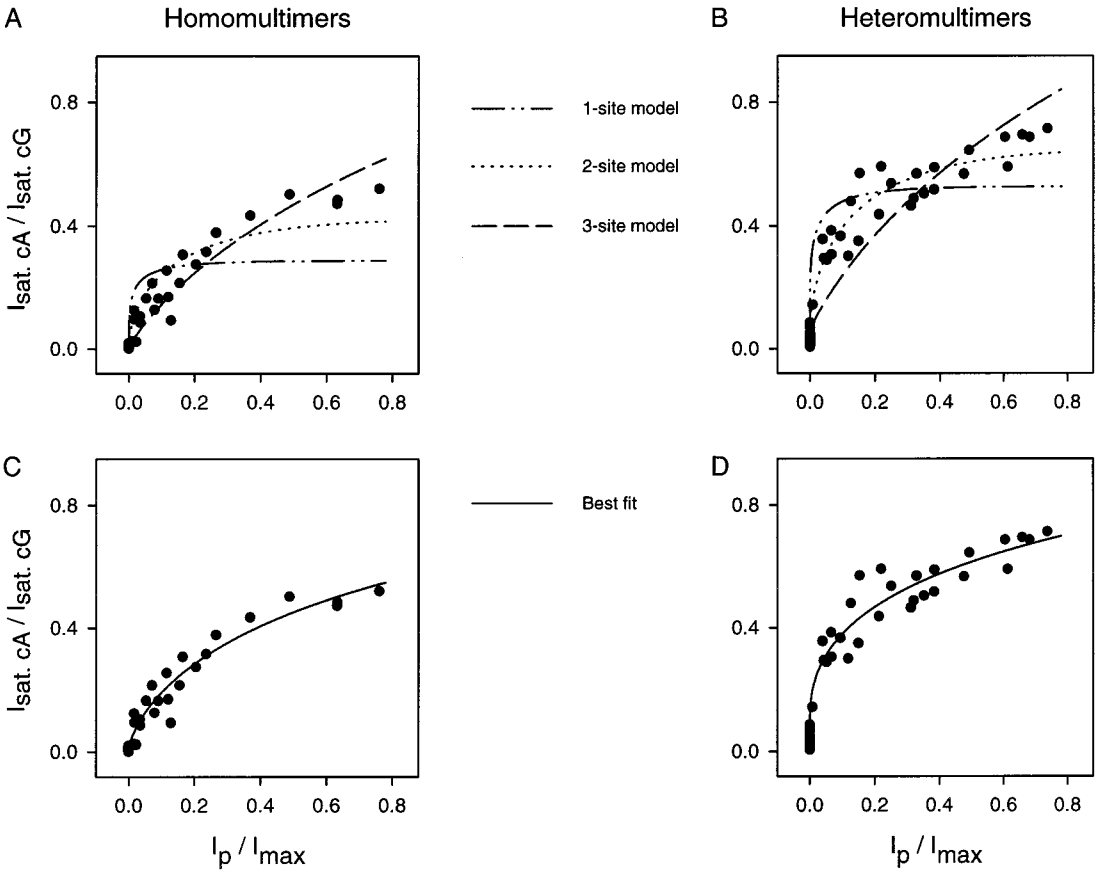

FIGURE 5: Quantifying the number of bound cGMP's required to make cAMP an effective agonist of rod CNG channels. Data are replotted from Figure 3A. The ratios between the current induced by saturating cAMP and the current induced by saturating cGMP ($I_{sat.\ cA}/I_{sat.\ cG}$) through homomeric (A, C) and heteromeric (B, D) channels are plotted against the level of covalent activation (I_p/I_{max}). See text for detailed explanations of each model. (A) 1-site model, $X = Y = Z = 28.8\%$; 2-site model, $X = 0.66\%$, $Y = Z = 41.9\%$; 3-site model, $X = Y = 0.66\%$, $Z = 71.3\%$. (B) 1-site model, $X = Y = Z = 52.6\%$; 2-site model, $X = 6.0\%$, $Y = Z = 64.1\%$; 3-site model, $X = Y = 6.0\%$, $Z = 96.1\%$. (C) Best fit, $X = 0.0\%$, $Y = 19.2\%$, $Z = 60.5\%$. (D) Best fit, $X = 24.8\%$, $Y = 38.7\%$, $Z = 74.7\%$.

where *X*, *Y*, and *Z* are the fractional currents induced by saturating cAMP (compared with saturating cGMP) through channels containing one, two, and three tethered cGMP's, respectively, and *a* is the fractional current induced by saturating cAMP through unliganded channels. Figure 5A and Figure 5B illustrate three limiting cases. The 1-site model assumes that significant cAMP activation occurs after at least one site is occupied by cGMP, and the fractional currents induced by saturating cAMP through singly, doubly, and triply cGMP-tethered channels are the same, i.e., $X = Y = Z$. The 2-site model assumes that significant cAMP activation occurs after at least two sites are occupied by cGMP, the fractional cAMP-induced currents through doubly and triply cGMP-tethered channels are the same, and the fractional cAMP-induced currents though unliganded and singly cGMP-tethered channels are the same, i.e., $X = a$, $Y = Z$. In the 3-site model, significant cAMP activation occurs only after at least three sites are occupied by cGMP, and the fractional cAMP-induced currents though unliganded, singly, and doubly cGMP-tethered channels are the same, i.e., $X = Y = a$. Figure 5C,D shows fits with eq 4 for homomeric and heteromeric channels, in which the values of *X*, *Y*, and *Z* were free to change in order to obtain the best possible fit.

The reduced chi-square (χ_v^2) test (see Materials and Methods) was used to judge the quality of fits in Figure 5. The calculated variances of $I_{sat.\ cA}/I_{sat.\ cG}$ were generally small (ranging from 0.001 to 0.01) and similar throughout all levels of covalent activation (Figure 6). Homomeric and heteromeric channels had comparable parent variances. In individual experiments, the error is usually a constant current (uncertainty in the leak current and maximal patch current),

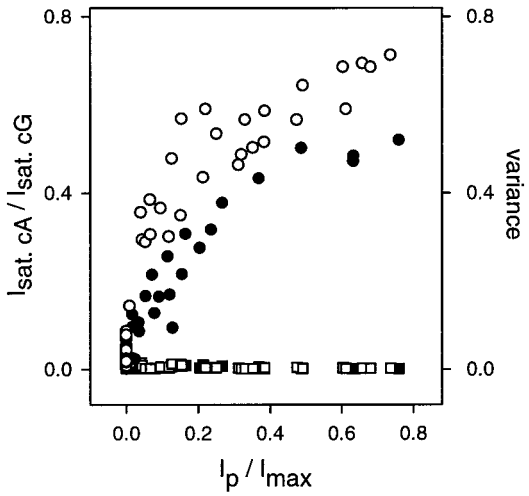

FIGURE 6: Variances of the ratios of the current induced by saturating cAMP and the current induced by saturating cGMP through homomeric (filled squares) and heteromeric (open squares) channels were comparable between groups, and similar atop all levels of covalent activation. The calculation of variance is described under Materials and Methods. The ratios of the current induced by saturating cAMP and the current induced by saturating cGMP are shown for comparison (same data and symbols as in Figure 3A).

instead of a percentage of the measured current. This would tend to give rise to a relatively uniform variance at different levels of covalent activation. However, patch-to-patch variability in activation parameters probably also contributed to the variance in ways that are harder to predict. For homomultimers, the 1-site model clearly did not fit the data in Figure 5A ($\chi_v^2 = 8.79$). Moreover, the value of X from the best fit in Figure 5C is 0% (close to the measured value of 0.7% in unliganded channels). Thus, it is unlikely that cAMP efficacy was significantly improved in singly cGMP-tethered homomeric channels. The 2-site and the 3-site models in Figure 5A fit the data somewhat better than the 1-site model, though neither of them provided a good fit ($\chi_v^2 = 2.07$ and 1.51, respectively). The best fit ($\chi_v^2 = 0.67$) was obtained with fractional cAMP-induced currents of 19.2% through doubly cGMP-tethered channels and 60.5% through triply cGMP-tethered channels (Figure 5C). This suggests that for α-subunit homomultimers, at least two sites must be occupied by cGMP for enhanced cAMP efficacy, and three sites must be occupied by cGMP for maximal cAMP efficacy (Figure 7A).

In the case of heteromultimers, the data did not discriminate between two models that could account for improved cAMP efficacy. Figure 5B shows that both the 1-site model ($\chi_v^2 = 3.90$) and the 3-site model ($\chi_v^2 = 3.59$) provided poor fits to the data. The 2-site model had a χ_v^2 value of 1.10. This value was close enough to 1.0 to be considered a good fit. In the 2-site model, with subunits labeled at random by APT-cGMP, having any two of the four binding sites of the heteromeric channel occupied by cGMP is sufficient to cause maximal cAMP efficacy (Figure 7B); in this scenario, singly cGMP-tethered heteromeric channels do not contribute to improved cAMP efficacy. However, the best fit ($\chi_v^2 = 0.87$) in Figure 5D suggests another possible scenario. The maximal cAMP-induced currents were 24.8% of the maximal cGMP-induced currents through singly cGMP-tethered channels, 38.7% through doubly cGMP-tethered channels, and 74.7% through triply cGMP-tethered channels. This suggests that in heteromultimers (Figure 7C), singly cGMP-tethered channels contribute somewhat to improved cAMP efficacy, doubly cGMP-tethered channels contribute more, and triply cGMP-tethered channels contribute the most ($X < Y < Z$).

β-N1201 Plays a Key Role in the Enhancement of cAMP Efficacy in Heteromeric Channels. We have attempted to pinpoint the residue(s) in the β subunit responsible for the increased efficacy with which cAMP opens heteromeric channels. As described earlier, D604 in α-subunit homomultimers, which is located near the end of the C-helix in the cyclic nucleotide-binding domain, has been shown to strongly influence the relative ability of different agonists to promote the allosteric conformational change associated with channel opening (*44*). In the β subunit, the corresponding amino acid (based on the alignment of primary sequences) is the neutral residue N1201. To test whether this residue is partly or solely responsible for the increased cAMP efficacy in heteromeric channels, we made the mutation N1201D. The responses of wild-type and mutant channels are compared in Figure 8 and Table 1. The Hill equation parameters n and $K_{1/2}$ for cGMP were not significantly altered by the mutation (the probability of opening of fully liganded channels was not measured). Strikingly, the efficacy of saturating cAMP (compared to saturating cGMP) was reduced from 6.0 to 1.4%. This was close to the value of 0.7% for homomultimers, although the difference was still significant. The mutation also reduced the relative efficacy of cIMP to a level that was indistinguishable from that observed in homomultimers (Figure 8B). Thus, for both partial agonists this single point mutation caused the resultant heteromultimers to behave more like wild-type homomultimers than wild-type heteromultimers. This demonstrates that N1201 is largely responsible for the higher activation efficacies of cAMP and cIMP in heteromultimers.

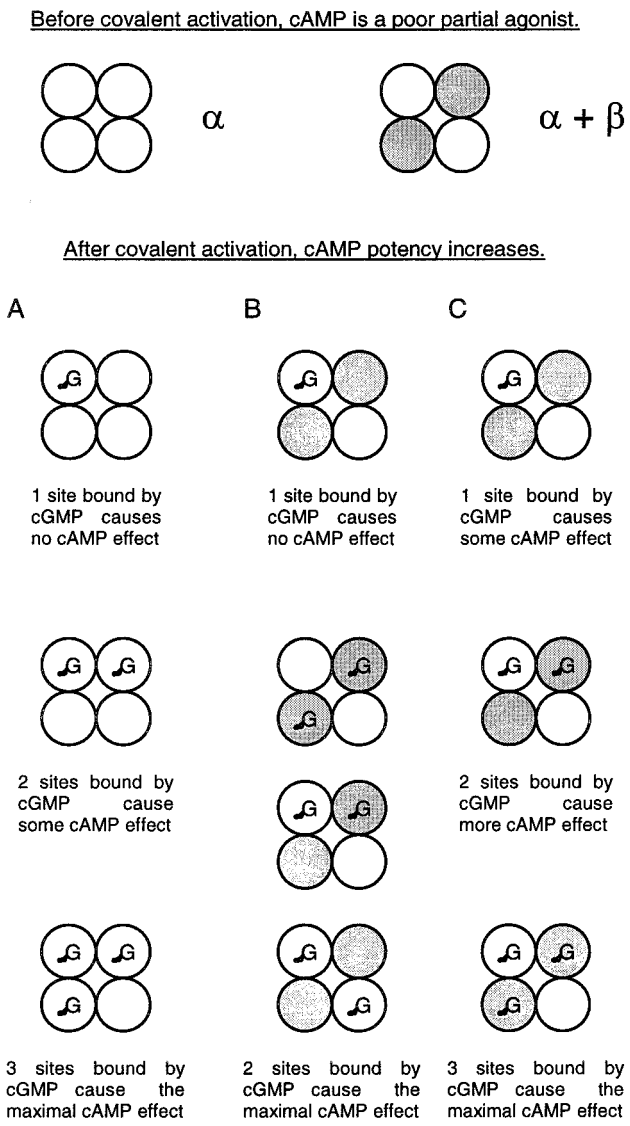

FIGURE 7: Models that account for improved cAMP efficacy of cGMP-tethered homomeric (A) and heteromeric (B and C) rod CNG channels. Open circles, α subunits; filled circles, β subunits. The subunit arrangement of heteromultimers is taken from He et al. (*27*). Subunits lacking tethered cGMP's are available for cAMP binding. For heteromultimers, panels B and C demonstrate two possible mechanisms (see text). Not all possible cGMP-primed channel types are shown.

DISCUSSION

cAMP Becomes an Effective Agonist of Rod CNG Channels Primed by the Binding of cGMP. The covalent tethering of cGMP moieties to rod CNG channels has allowed us to study activation by defined combinations of a full agonist (cGMP) and a partial agonist (cAMP). The conventional

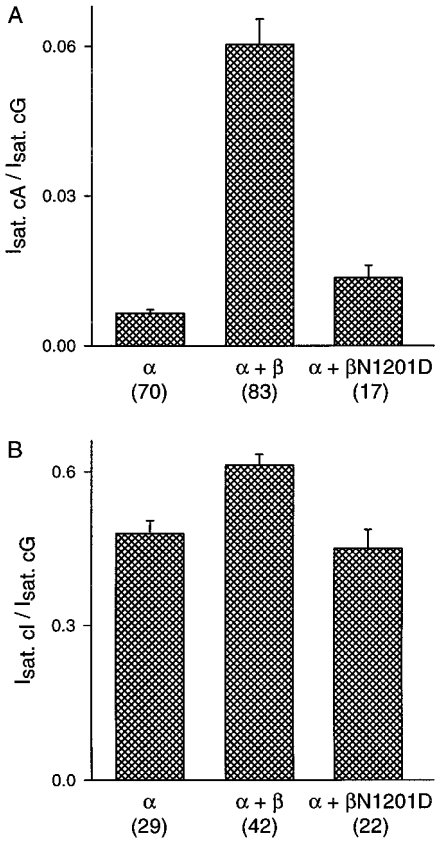

FIGURE 8: Comparison of responses of different channel constructs to partial agonists. Bars are expressed as mean ± SEM. Number of experiments is indicated in parentheses under each construct. (A) Ratios of the current induced by saturating cAMP and the current induced by saturating cGMP ($I_{sat.\ cA}/I_{sat.\ cG}$). The maximal cAMP responses among all three constructs were statistically different ($p < 0.01$, Student's *t*-test). (B) Ratios of the current induced by saturating cIMP and the current induced by saturating cGMP ($I_{sat.\ cI}/I_{sat.\ cG}$). Only the maximal cIMP responses between α and α + *β* and between α + *β* and α + *β*-N1201D were different ($p < 0.01$).

approach to this problem is to study mixtures of free cGMP and cAMP, but competition makes it very difficult to know the precise occupancy by each ligand. The results indicate that cAMP, which activated only a small percentage of channels on its own, became an effective agonist (maximally activating 50% of the remaining current in homomultimers and 70% in heteromultimers) when the channels were partially occupied by cGMP. In general, there was a progressive increase in the efficacy of cAMP with increasing numbers of tethered cGMP's, and heteromeric channels were effectively primed by fewer cGMP's than homomeric channels.

The data suggest that cAMP has an appreciable effect on homomeric channels (19% of the current activated by cGMP) once two cGMP's are bound, and a much larger effect (61%) when three cGMP's are bound. For heteromeric channels, where cAMP is a more effective partial agonist to begin with, the data did not discriminate between two models: (1) two cGMP's are both necessary and sufficient for high cAMP efficacy (64%), and (2) there is a progressive increase in cAMP efficacy with each cGMP that binds (25, 39, and 75% with one, two, and three cGMP's bound). These two mechanisms differ somewhat quantitatively, but they both indicate that cAMP can be quite effective in heteromeric channels with two cGMP's bound, in contrast to homomeric channels. A comparison of fits of the 2-site model to data from homomultimers and heteromultimers in Figure 5A,B also illustrates the point.

Previous studies have shown that the *β* subunits are responsible for the higher cAMP efficacy in heteromeric channels (*21*, *22*). In broad agreement with the second study, we found that *β*-N1201 has a crucial role in the higher efficacy. Changing that residue to aspartic acid (the corresponding residue in homomeric channels) significantly reduced cAMP efficacy at saturating concentrations. In our experiments, the reduction was more dramatic, such that the mutant channel had a cAMP efficacy closer to that observed in homomeric channels. There were two differences in the experimental conditions that may be pertinent: we expressed a full-length *β* subunit (*18*) while Pages et al. (*22*) used a version in which the N-terminus was truncated at position 571; we used symmetrical Na^+ solutions while they used symmetrical K^+ solutions (for one of their constructs, α-D604N homomultimers, the probability of opening was measurably lower in symmetrical Na^+ than in symmetrical K^+). Nonetheless, these results agree with earlier work showing that the nature of this residue in different CNG channel subunits has a dominant role in nucleotide specificity (*44*).

Simple Allosteric Mechanisms Can Account for the Priming Effect of cGMP. Because cAMP is a poor agonist, the cGMP priming effect from neighboring subunits is certainly an indication of cooperativity, i.e., strong interactions between subunits in channel activation. However, these results do not serve as a critical test for different allosteric models of channel activation. Historically, steady-state data have not been used to distinguish between allosteric models. For example, the simple Hill model provides an excellent fit to most steady-state dose−response data. Although covalent tethering of cGMP moieties affords a higher resolution of liganded states than is typical in most steady-state experiments, there is not enough precision in the current data to evaluate different allosteric models (based on the different empirical models that can fit the heteromultimer data in Figure 5B,D). However, it is important to point out that the basic priming effects of cGMP on cAMP efficacy can be accounted for by a variety of allosteric mechanisms. For example, the Monod−Wyman−Changeux concerted model (*60*), although it has been shown to be too simple to explain the activation of CNG channels (*26*, *32*, *33*), can account for the basic phenomenon of a good agonist priming a channel to be activated by a poor agonist. In this model, the channel exists in either a closed (T) or an open (R) state. In the absence of ligand, the equilibrium strongly favors the closed state; the equilibrium constant, $L = [T]/[R]$, can be estimated from single channel experiments to be about 6.7×10^5 (*26*). The ligand binds more tightly to the open state (the dissociation constant $K_R < K_T$). As a result, the binding of each ligand decreases the equilibrium constant for channel closing by a constant factor, $c = K_R/K_T$. At saturating ligand concentrations, and assuming a tetrameric channel, the fraction of open channels is given by

$$F = 1/(1 + Lc^4) \quad (5)$$

In homomeric channels, saturating cGMP causes the channel

to be open 95% of the time (*26*, *32*), and saturating cAMP under the same experimental conditions causes about 0.7% opening (Table 1). From these data, different c values can be calculated from eq 5: $c_{cG} = 0.030$ and $c_{cA} = 0.22$. Equation 5 can be modified to account for activation by mixtures of cGMP and cAMP:

$$F = 1/(1 + L \times {c_{cG}}^{x} \times {c_{cA}}^{4-x}) \quad (6)$$

where x is the number of binding sites containing covalently tethered cGMP's. It follows that atop a certain number of covalently attached ligands, the ratio of currents in saturating cAMP and saturating cGMP is given by

$$I_{sat.\ cA}/I_{sat.\ cG} = [1/(1 + L \times {c_{cG}}^{x} \times {c_{cA}}^{4-x}) - 1/(1 + L \times {c_{cG}}^{x})]/[1/(1 + L \times {c_{cG}}^{4}) - 1/(1 + L \times {c_{cG}}^{x})] \quad (7)$$

At high levels of covalent activation ($I_p/I_{max} \geq 0.75$), it has been shown that, aside from fully liganded channels that do not respond to free cyclic nucleotide, the predominant form of the channel is triply liganded (*52*). Equation 7 can be used to calculate the effect of saturating cAMP on channels containing three covalently tethered cGMP's ($x = 3$), yielding an $I_{sat.\ cA}/I_{sat.\ cG}$ value of 0.60. This agrees reasonably well with the experimental value obtained at high I_p/I_{max} in Figure 5A. Similarly, by expanding the simple concerted model to allow different c values for α and β subunits (e.g., a lower c value for cAMP binding to the β subunit), the model can approximate the data at high I_p/I_{max} values in Figure 5B. Concerted models imply that the binding of a particular ligand changes the equilibrium constant for opening by a constant factor, and therefore makes a constant energetic contribution to opening. Thus, cAMP binding would impart the same amount of energy before or after cGMP binds. The priming effect arises because cGMP significantly lowers the energy barrier for opening, making cAMP an effective agonist.

A complete understanding of the interactions between cGMP and cAMP will require the measurement of dose−response relations at each level of covalent activation, and the measurement of kinetic transitions at the single channel level. It would also be useful to have a method for covalently tethering agonists to particular subunits. A recent study with cGMP affinity labels is an advance in that direction (*61*). Based on the current data, we cannot completely account for the earlier observations that low concentrations of cAMP potentiated cGMP-induced currents through native, heteromeric channels (*49*, *50*), but not through homomeric channels (*22*). This would require knowing all of the apparent ligand affinities. Nonetheless, the difference is likely due, at least in part, to the fact that fewer cGMP's are required to prime heteromeric channels. When cAMP binds to unoccupied sites and competes with cGMP at other sites in heteromultimers, the net effect is an increase in current. Competition between cAMP and cGMP is not deleterious in heteromultimers, because cAMP is an effective agonist with fewer sites occupied by cGMP.

Possible Physiological Significance of the Synergistic Interaction between cAMP and cGMP. To our knowledge, there is no firmly established role for cAMP in phototransduction. However, cAMP and cGMP are known to coexist in all of the tissues or cell types in which CNG channels have been identified. The list includes olfactory receptor neurons, pinealocytes, retinal interneurons, sympathetic neurons, hippocampal neurons, heart, aorta, kidney, testes, liver, and skeletal muscle (*6*−*9*). In most of these settings, the physiological roles of the channel are not known. As mentioned earlier, there is a fascinating gradation of specificities for cGMP and cAMP among the known CNG channel subunits. Here we have shown that cAMP can significantly activate heteromeric rod channels, considered to be highly cGMP-specific, if they are first primed by the binding of cGMP. Taken together, these observations make it likely that the two cyclic nucleotides will act synergistically on CNG channels in many cell types.

ACKNOWLEDGMENT

We thank Drs. Ambarish Ghatpande and Thomas Rich for helpful discussions. The cDNAs encoding the bovine retinal rod CNG channel α and β subunits were kindly provided by Dr. William Zagotta (University of Washington School of Medicine, Seattle, WA) and Dr. Robert Molday (University of British Columbia, Vancouver, BC), respectively. L-*cis*-diltiazem was the gift of Dr. King-Wai Yau (Johns Hopkins University School of Medicine, Baltimore, MD).

REFERENCES

1. Fesenko, E. E., Kolesnikov, S. S., and Lyubarsky, A. L. (1985) *Nature 313*, 310−313.
2. Haynes, L., and Yau, K. W. (1985) *Nature 317*, 61−64.
3. Yau, K. W., and Baylor, D. A. (1989) *Annu. Rev. Neurosci. 12*, 289−327.
4. Nakamura, T., and Gold, G. H. (1987) *Nature 325*, 442−444.
5. Schild, D., and Restrepo, D. (1998) *Physiol. Rev. 78*, 429−466.
6. Kaupp, U. B. (1995) *Curr. Opin. Neurobiol. 5*, 434−442.
7. Finn, J. T., Grunwald, M. E., and Yau, K. W. (1996) *Annu. Rev. Physiol. 58*, 395−426.
8. Wei, J. Y., Roy, D. S., Leconte, L., and Barnstable, C. J. (1998) *Prog. Neurobiol. 56*, 37−64.
9. Biel, M., Zong, X., and Hofmann, F. (1999) *Adv. Second Messenger Phosphoprotein Res. 33*, 231−250.
10. Tanaka, J. C., Eccleston, J. F., and Furman, R. E. (1989) *Biochemistry 28*, 2776−2784.
11. Gavazzo, P., Picco, C., Maxia, L., and Menini, A. (1996) in *Ionic Channels, Neurons, and the Brain* (Torre, V., and Conti, F., Eds.) pp 75−83, Plenum Press, New York.
12. Cook, N. J., Hanke, W., and Kaupp, U. B. (1987) *Proc. Natl. Acad. Sci. U.S.A. 84*, 585−589.
13. Kaupp, U. B., Niidome, T., Tanabe, T., Terada, S., Bonigk, W., Stuhmer, W., Cook, N. J., Kangawa, K., Matsuo, H., Hirose, T., Miyata, T., and Numa, S. (1989) *Nature 342*, 762−766.
14. Cook, N. J., Molday, L. L., Reid, D., Kaupp, U. B., and Molday, R. S. (1989) *J. Biol. Chem. 264*, 6996−6999.
15. Molday, L. L., Cook, N. J., Kaupp, U. B., and Molday, R. S. (1990) *J. Biol. Chem. 265*, 18690−18695.
16. Molday, R. S., Molday, L. L., Dose, A., Clark-Lewis, I., Illing, M., Cook, N. J., Eismann, E., and Kaupp, U. B. (1991) *J. Biol. Chem. 266*, 21917−21922.
17. Chen, T. Y., Peng, Y. W., Dhallan, R. S., Ahamed, B., Reed, R. R., and Yau, K. W. (1993) *Nature 362*, 764−767.
18. Korschen, H. G., Illing, M., Seifert, R., Sesti, F., Williams, A., Gotzes, S., Colville, C., Muller, F., Dose, A., Godde, M., Molday, L., Kaupp, U. B., and Molday, R. S. (1995) *Neuron 15*, 627−636.
19. Colville, C. A., and Molday, R. S. (1996) *J. Biol. Chem. 271*, 32968−32974.

20. Ardell, M. D., Aragon, I., Oliveira, L., Porche, G. E., Burke, E., and Pittler, S. J. (1996) *FEBS Lett. 389*, 213−218.
21. Shammat, I. M., and Gordon, S. E. (1999) *Neuron 23*, 809−819.
22. Pages, F., Ildefonse, M., Ragno, M., Crouzy, S., and Bennett, N. (2000) *Biophys. J. 78*, 1227−1239.
23. Gordon, S. E., and Zagotta, W. N. (1995) *Proc. Natl. Acad. Sci. U.S.A. 92*, 10222−10226.
24. Varnum, M. D., and Zagotta, W. N. (1996) *Biophys. J. 70*, 2667−2679.
25. Liu, D. T., Tibbs, G. R., and Siegelbaum, S. A. (1996) *Neuron 16*, 983−990.
26. Ruiz, M. L., and Karpen, J. W. (1997) *Nature 389*, 389−392.
27. He, Y., Ruiz, M., and Karpen, J. W. (2000) *Proc. Natl. Acad. Sci. U.S.A. 97*, 895−900.
28. Brown, R. L., Gerber, W. V., and Karpen, J. W. (1993) *Proc. Natl. Acad. Sci. U.S.A. 90*, 5369−5373.
29. Brown, R. L., Gramling, R., Bert, R. J., and Karpen, J. W. (1995) *Biochemistry 34*, 8365−8370.
30. Weber, I. T., and Steitz, T. A. (1987) *J. Mol. Biol. 198*, 311−326.
31. Su, Y., Dostmann, W. R., Herberg, F. W., Durick, K., Xuong, N. H., Ten Eyck, L., Taylor, S. S., and Varughese, K. I. (1995) *Science 269*, 807−813.
32. Liu, D. T., Tibbs, G. R., Paoletti, P., and Siegelbaum, S. A. (1998) *Neuron 21*, 235−248.
33. Ruiz, M., and Karpen, J. W. (1999) *J. Gen. Physiol. 113*, 873−895.
34. Ruiz, M., Brown, R. L., He, Y., Haley, T. L., and Karpen, J. W. (1999) *Biochemistry 38*, 10642−10648.
35. Haynes, L. W., Kay, A. R., and Yau, K. W. (1986) *Nature 321*, 66−70.
36. Zimmerman, A. L., and Baylor, D. A. (1986) *Nature 321*, 70−72.
37. Matthews, G. (1998) in *Ion Channel Pharmacology* (Soria, B., and Cena, V., Eds.) pp 383−396, Oxford University Press, New York.
38. Dhallan, R. S., Yau, K. W., Schrader, K. A., and Reed, R. R. (1990) *Nature 347*, 184−187.
39. Liman, E. R., and Buck, L. B. (1994) *Neuron 13*, 611−621.
40. Bradley, J., Li, J., Davidson, N., Lester, H. A., and Zinn, K. (1994) *Proc. Natl. Acad. Sci. U.S.A. 91*, 8890−8894.
41. Sautter, A., Zong, X., Hofmann, F., and Biel, M. (1998) *Proc. Natl. Acad. Sci. U.S.A. 95*, 4696−4701.
42. Bonigk, W., Bradley, J., Muller, F., Sesti, F., Boekhoff, I., Ronnett, G. V., Kaupp, U. B., and Frings, S. (1999) *J. Neurosci. 19*, 5332−5347.
43. Frings, S., Lynch, J. W., and Lindemann, B. (1992) *J. Gen. Physiol. 100*, 45−67.
44. Varnum, M. D., Black, K. D., and Zagotta, W. N. (1995) *Neuron 15*, 619−625.
45. Gordon, S. E., Oakley, J. C., Varnum, M. D., and Zagotta, W. N. (1996) *Biochemistry 35*, 3994−4001.
46. Sunderman, E. R., and Zagotta, W. N. (1999) *J. Gen. Physiol. 113*, 621−640.
47. Shapiro, M. S., and Zagotta, W. N. (2000) *Biophys. J. 78*, 2307−2320.
48. Scott, S. P., and Tanaka, J. C. (1998) *Biochemistry 37*, 17239−17252.
49. Furman, R. E., and Tanaka, J. C. (1989) *Biochemistry 28*, 2785−2788.
50. Ildefonse, M., Crouzy, S., and Bennett, N. (1992) *J. Membr. Biol. 130*, 91−104.
51. Karpen, J. W., Ruiz, M., and Brown, R. L. (2000) *Methods Enzymol. 315*, 755−772.
52. Karpen, J. W., and Brown, R. L. (1996) *J. Gen. Physiol. 107*, 169−181.
53. Liman, E. R., Tytgat, J., and Hess, P. (1992) *Neuron 9*, 861−871.
54. Zimmerman, A. L., Karpen, J. W., and Baylor, D. A. (1988) *Biophys. J. 54*, 351−355.
55. Stern, J. H., Kaupp, U. B., and MacLeish, P. R. (1986) *Proc. Natl. Acad. Sci. U.S.A. 83*, 1163−1167.
56. Quandt, F. N., Nicol, G. D., and Schnetkamp, P. P. M. (1991) *Neuroscience 42*, 629−638.
57. Molokanova, E., Trivedi, B., Savchenko, A., and Kramer, R. H. (1997) *J. Neurosci. 17*, 9068−9076.
58. Bevington, P. R. (1969) *Data Reduction and Error Analysis for the Physical Sciences*, McGraw-Hill, New York.
59. Taylor, W. R., and Baylor, D. A. (1995) *J. Physiol. 483*, 567−582.
60. Monod, J., Wyman, J., and Changeux, J.-P. (1965) *J. Mol. Biol. 12*, 88−118.
61. Brown, R. L., Haley, T. L., and Snow, S. D. (2000) *Biochemistry 39*, 432−441.

BI002014N